Applied Catalysis B: Environmental 180 (2016) 330–335

Contents lists available at ScienceDirect

Applied Catalysis B: Environmental

journal homepage: www.elsevier.com/locate/apcatb

Effect of water matrix on photocatalytic degradation and general kinetic modeling

Nerea Rioja[a,b], Saioa Zorita[b], Francisco J. Peñas[a,*]

[a] Department of Chemistry and Soil Science, University of Navarra, 31008 Pamplona, Spain
[b] Tecnalia-Energy and Environment Division, c/ Geldo, Parque Tecnológico de Bizkaia, Edificio 700, 48160 Derio, Spain

ARTICLE INFO

Article history:
Received 13 April 2015
Received in revised form 17 June 2015
Accepted 19 June 2015
Available online 25 June 2015

Keywords:
Clofibric acid photodegradation
Inorganic salts
Organic matter
Environmental water
Kinetic modeling

ABSTRACT

Photocatalysis employing TiO_2 nanoparticles was studied to assess the effect of aqueous matrix nature in the degradation of clofibric acid (CFA) under UV-A radiation. Aeroxide TiO_2-P25 at 0.50 g/L was the most effective catalyst among those tested, with a CFA degradation of 98.5% after 15 min. The CFA photodegradation in environmental waters (tap, mineral, river and recycled wastewater) and in the presence of inorganic (NaCl, $FeCl_3$, $FeCl_2$, $AlCl_3$, $CaCl_2$, $Al_2(SO_4)_3$, $Fe_2(SO_4)_3$, Na_2SO_4, $NaHCO_3$, and Na_2CO_3) and organic compounds (humic acids, and a surfactant) commonly found in real waters was compared to that obtained in pure water. In general, the removal efficiency decreased with inorganic salts, especially with sulfates and carbonates (>70% deactivation), and also in environmental waters (>90%). A general kinetic model has been developed to describe the CFA photodegradation depending on the type and concentration of substances present in water. The first-order kinetic constants were estimated by defining a characteristic parameter for each ion species tested in the aqueous matrix. High correlation ($R^2 > 0.99$ in most cases) was observed between experimental CFA concentrations and those predicted by the model.

1. Introduction

In the last couple of decades the advances in water quality analytical techniques has led to an increased focus on water micropollutants and emerging contaminants such as pharmaceuticals [1–5]. The presence of therapeutic drugs in the aquatic environment is becoming widespread [5–8], mainly because actual wastewater treatment plants (WWTP) fail on a quantitative removal of many of these pollutants [9–11]. Furthermore, due to the expected scarcity of freshwater resources, there is an increasing need on high quality recycled water.

On the other hand, despite the fact that heterogeneous photocatalysis has been studied for some years now, it is still considered a promising treatment technology for eliminating organic micropollutants from water [12–14]. Its attractiveness relies on its ability to degrade organic chemicals into innocuous end products. Among the organic compounds that have been degraded in water by heterogeneous photocatalysis, dyes, pharmaceuticals, phenols plus many other pollutants are found [15–18]. However, one of the major limitations is that actual catalysts lack of high quantum yields mainly due to the fast recombination of the photogenerated electrons and holes after excitation [19]. In fact, typical quantum yields are often below 10%, although a maximum of 40% has been reported [19,20]. This decrease in degradation efficiency is generally due to intrinsic and extrinsic factors [21]. The first ones are related to the system design and catalyst type while the others are linked to the aqueous matrix (i.e. pH, structure and concentration of pollutant, ionic composition, and presence of impurities) [15,19].

Although the photocatalytic technology is aimed for environmental applications, most of the studies are conducted in pure water, and little is known about its performance using real matrices (such as tap, river, or recycled water). Some studies found that inorganic ions can significantly diminish the photocatalytic efficiency [22,23], being this effect primarily attributed to the adsorption of ions on TiO_2 surface [24]. The effect of wastewater matrices on photocatalytic degradation of pollutants has been little studied, showing lower removal rates than those with pure water [25–29]. This efficiency decrease has been largely attributed to the quenching of radicals by salts and organic matter [25]. However, for the further development of this technology, more studies on how water components affect photocatalysis are required.

This work addresses the effect of water matrix nature on photocatalytic degradation of emerging contaminants in water, using clofibric acid (CFA) as the target pollutant. The kinetics of CFA photocatalytic oxidation in various environmental waters (mineral, tap, river, and recycled water) has been determined for several

* Corresponding author. Fax: +34 948 425600.

http://dx.doi.org/10.1016/j.apcatb.2015.06.038
0926-3373/

Table 1
Main features of the commercial photocatalysts.

	Kertak TiO_2-nanofibres	Aeroxide TiO_2 P25	Aeroxide TiO_2 P90	Microsphere photospheres
Diameter or length (μm)[a]	0.295 ± 0.070	0.021–0.025	0.014	45
Surface area (m^2/g)[a]	98.7	50	90–100	–
Crystallinity[a]	100% Anatase	80% Anatase, 20% Rutile	90% Anatase, 10% Rutile	–

[a] Information provided by the manufacturers.

catalyst types (Aeroxide TiO_2 powder P25 and P90, Photospheres, Kertak TiO_2 nanofibres, and TiO_2–SiO_2 composite), and for different concentrations of organic (sodium *n*-octyl-sulfate, and humic acid) and inorganic (NaCl, $FeCl_3$, $FeCl_2$, $AlCl_3$, $Fe_2(SO_4)_3$, $Al_2(SO_4)_3$, Na_2SO_4, Na_2CO_3, $NaHCO_3$, and $CaCl_2$) compounds. A new kinetic model for predicting the photodegradation efficiency of CFA in different water samples has been developed by introducing a parameter characteristic of each substance used to form the respective aqueous matrix.

2. Experimental

2.1. Photocatalytic materials and water matrices

Titanium dioxide Aeroxide P25 and P90 were acquired from Evonik (Germany), Photospheres from Microsphere Technology (Ireland), and TiO_2 nanofibres from Kertak Nanotechnology (Czech Republic). A batch of TiO_2–SiO_2 particles were prepared according to the method of Jafry et al. [30]. The available features of the four commercial photocatalysts assayed are given in Table 1.

Deionized water was obtained from a purification system (Millipore Milli-Q, USA). Bottled mineral water (pH 7.5, conductivity 521 μS/cm, TOC <0.2 mg/L) was purchased at a local supermarket. Tap water (pH 7.9, conductivity 232 μS/cm, TOC 2.2 mg/L) was obtained from the local drinking water supply. The river water matrix (pH 8.13, conductivity 509 μS/cm, TOC 4.7 mg/L) was collected from the Asua river (Spain). The recycled wastewater matrix consisted of the filtrate (Whatman GF/F 0.7 μm, Germany) of treated sewage water (pH 7.54, conductivity 818 μS/cm, TOC 27.1 mg/L) collected from the Zumaia WWTP effluent (Spain).

2.2. Photocatalytic experiments

Batch experiments were carried out in 150-mL reaction cells under UV-A light irradiation (365 nm, 0.89 mW/cm^2). An UV-A lamp (GE Lighting, F20T12/BL 20W, USA), with a spectral a peak of 367 nm, was used as the source light. The scheme of the experimental setup is shown in the supplementary material (Fig. A.1). The radiation intensity was measured inside of the reactor using a UV-A radiometer (Lutron, Taiwan) located at the bottom of the vessel. In each assay, an enough amount of the corresponding photocatalytic material to typically give 50 mg of TiO_2 was suspended in 100-mL of pure water (i.e. 500 mg-TiO_2/L) and spiked with the target drug (clofibric acid, 1.00 μg/mL) and other compounds when necessary. Some environmental waters were used as aqueous matrix in other experimental series. Each test was conducted in triplicate, keeping the first 60 min in darkness for adsorption and then the next 15 min for photocatalytic degradation. The previous essays carried out in darkness showed a low CFA adsorption within 60 min (5.7 ± 0.9%). Aliquots of 0.6 mL were periodically sampled from reaction cells, and then centrifuged at 4500 rpm for 30 min (Sigma Laborzentrifugen, 4–15, Germany) to remove the photocatalyst particles before analysis.

2.3. Analytical methods

The concentration of clofibric acid was measured in triplicate by HPLC. More details can be found elsewhere [29]. A conductivity meter (Hanna Instruments, HI9835, Spain) was employed to determine the conductivity and NaCl content of the samples. A portable instrument (Mettler-Toledo, SevenGo SG2, Switzerland) was used to measure and control pH in samples. Particle size and zeta potential were measured by electrophoretic light scattering (Malvern Instruments, Zetasizer Nano-ZS, UK), at 25 °C, and using a high-concentration cell (Malvern Instruments, ZEN1010, UK). For each water matrix, suspensions of the photocatalytic particles (0.50 g-TiO_2/L unless otherwise stated) were stirred at 700 rpm for at least 2 min prior to taking the samples for measurements. All of the non-linear regression parameters were obtained by minimizing the sum of the squared difference between the experimental and calculated data using the Solver add-in (Microsoft, Excel 2010, USA).

2.4. Reagents

Clofibric acid, iron(III) chloride hexahydrate, iron(II) chloride tetrahydrate, aluminium chloride hexahydrate, sodium sulfate, sodium carbonate, sodium bicarbonate, humic acid sodium salt [CAS 68131-04-4], hydrochloric acid (37%), sodium hydroxide, and sodium phosphate monobasic were obtained from Sigma-Aldrich (Germany). Sodium chloride, iron(III) sulphate hydrate (75%), aluminium sulfate octadecahydrate, and acetonitrile were purchased from Panreac (Spain). Sodium *n*-octylsulfate was supplied by Alfa Aesar (Germany). All reagents were used as received.

3. Results and discussion

3.1. Effect of photocatalyst type and dosage

Since activity of heterogeneous catalysts depends, among others, on particle size and crystalline structure, preliminary experiments were conducted with five TiO_2 catalysts in order to find the most suitable form for maximal performance. The CFA degradation profiles obtained (C/C_0 vs t) are depicted in Fig. 1. The error bars are the standard deviation of the mean for 3 batches. The photocatalytic degradation of CFA was well described by a pseudo-first-order kinetics, being this pattern also observed in the remaining experiments. As clearly shown, Aeroxide P25 and P90 were found to be highly active for CFA degradation (more than 95% after 15 min) in comparison with titania–P25/silica particles (51%), whereas the removal efficiencies were less than 10% for both Kertak nanofibres and Photospheres. Thus, as Aeroxide TiO_2–P25 showed the best performance in CFA removal, this nanoparticle photocatalyst was employed henceforth.

In general, photodegradation rate increases with catalyst loading until a maximum beyond which efficiency drops off because of the higher turbidity reduces the penetration of light through water. Therefore, additional experiments were conducted with TiO_2–P25 to determine the optimal catalyst loading for CFA degradation. As observed in Fig. 2a, loads of 500 and 1000 mg-TiO_2/L yielded virtually the same degradation profiles, whilst the CFA removal rate was significantly lower at 200 mg-TiO_2/L. The kinetic constant obtained

Table 2
Photodegradation of clofibric acid with Aeroxide P25 (500 mg/L) in presence of different substances.

Species	S (mg/L)	pH (−)	Z (mV)	d (nm)	k (min^{-1})	Species	S (mg/L)	pH (−)	Z (mV)	d (nm)	k (min^{-1})
Water	–	5.0	30.4	425	0.347	$Al_2(SO_4)_3$	50	4.5	17.0	4650	0.011
NaCl	30	5.3	−5.1	5370	0.145		170	4.3	13.6	4685	0.005
	500	5.6	−9.7	3780	0.050		200	4.2	13.4	4700	0.004
	5000	5.7	−6.0	3930	0.086	$Fe_2(SO_4)_3$	50	3.1	11.9	3550	0.009
	10000	5.7	−3.9	4080	0.169		200	2.9	8.9	5370	0.005
	20000	5.8	−6.8	3700	0.234	Na_2SO_4	20	5.1	10.3	5240	0.023
	30000	5.9	−2.7	4640	0.316		50	5.3	9.4	3830	0.019
$FeCl_3$	50	3.3	39.9	323	0.175		70	5.1	8.2	3910	0.018
	135	3.3	40.0	395	0.103		200	5.4	5.2	3590	0.010
	200	2.8	40.1	426	0.061	$NaHCO_3$	50	7.8	−21.9	4215	0.006
	500	2.6	37.4	347	0.056		200	7.9	−29.0	1980	0.010
$FeCl_2$	50	5.2	44.1	348	0.122		500	8.3	−34.3	1600	0.005
	100	5.1	44.0	352	0.098	Na_2CO_3	50	10.7	−42.9	543	0.001
	200	4.8	43.4	369	0.066	SOS	2	6.0	28.2	406	0.259
$AlCl_3$	20	4.9	35.8	390	0.421		5	6.1	22.4	379	0.239
	50	4.4	47.1	403	0.381		15	6.1	27.6	381	0.156
	120	4.1	47.0	382	0.331	HAS	1	6.1	−16.4	697	0.219
	200	4.2	46.7	343	0.270		3	6.5	−24.6	630	0.108
	500	3.9	49.7	396	0.221		5	6.6	−29.1	494	0.076
$CaCl_2$	75	5.3	N.A.	N.A.	0.097						

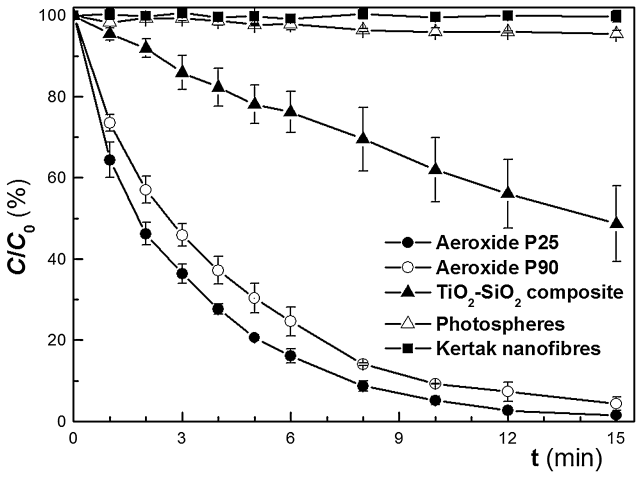

Fig. 1. Degradation profiles of CFA for different TiO_2 catalysts.

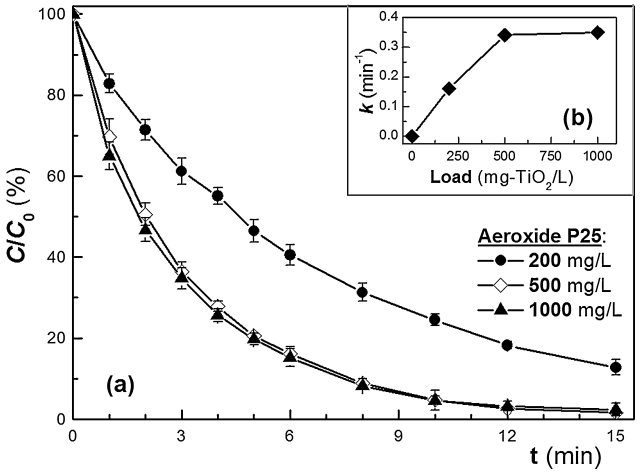

Fig. 2. Degradation of CFA for TiO_2-P25 in pure water: (a) Removal profiles; (b) Dependence of kinetic constant with catalyst loading.

at 500 mg/L was even slightly higher than that found at 1000 mg/L (Fig. 2b). Consequently, a concentration of 500 mg-TiO_2/L was chosen in subsequent experiments.

Table 3
Photodegradation of clofibric acid with Aeroxide P25 (500 mg/L) in different aqueous matrices.

Matrix	pH (−)	Z (mV)	d (nm)	k (min^{-1})
Pure water	5.0	30.4	425	0.3468
Bottled mineral water	5.8	−1.3	4490	0.0057
Tap water	6.4	−12.2	2550	0.0033
River water	6.6	−8.4	5510	0.0040
Recycled wastewater	7.5	−18.1	2580	0.0005

3.2. Effect of water matrix

As previously mentioned, Aeroxide P25 at 500 mg-TiO_2/L was used in all of the following experiments. The concentrations of the compounds tested (S), the pH of solutions, the measured zeta potential values (Z), the mean sizes of the catalyst aggregates (d), and the corresponding calculated kinetic constants (k) are given in Table 2. Similar information is listed in Table 3 for environmental waters. Note that k values were determined for each data set separately (substance and concentration), with a high correlation ($R^2 > 0.99$ in most cases). In general, significant TiO_2 deactivation by addition of inorganic salts or organic matter to water was quite evident. It is noteworthy that $AlCl_3$ was the only compound tested that, at its low concentrations, produced a positive effect on CFA photodegradation with regard to pure water. For instance, an increase in k of about 22% was observed for 20 mg-$AlCl_3$/L. Stable dispersions (in practice, $Z > 20$ mV, and aggregate sizes comparable to those of pure water) were obtained with aqueous solutions of $FeCl_3$, $FeCl_2$, $AlCl_3$, and SOS. Although the stability of catalyst suspensions is related to the size of aggregates formed, which is in turn linked to the surface charge of such particles, no relationships were found between these parameters (pH, Z, d, and k), with the only exception of a significant negative correlation between pH and Z ($r = -0.764$; $p < 0.001$). In fact, using the data from Tables 2 and 3, the point of zero charge (pzc) was estimated as 6.23, which is close to the accepted value for TiO_2 nanoparticles (pzc = 6.5).

Furthermore, in heterogeneous photocatalysis, changes in pH will result in changes in the charges of TiO_2 and substrate and in the size of catalyst aggregates, all leading to different adsorption behaviors and hence dissimilar degradation rates [31]. Note that CFA exists mostly in its ionized form ($C_6H_4CH_3COO^-$) at pH higher than its pK_a (i.e., 3.2), and also catalyst surface becomes positively charged below the point of zero charge of TiO_2 (pzc = 6.5). Therefore, optimal pH for CFA adsorption onto TiO_2 surface should be

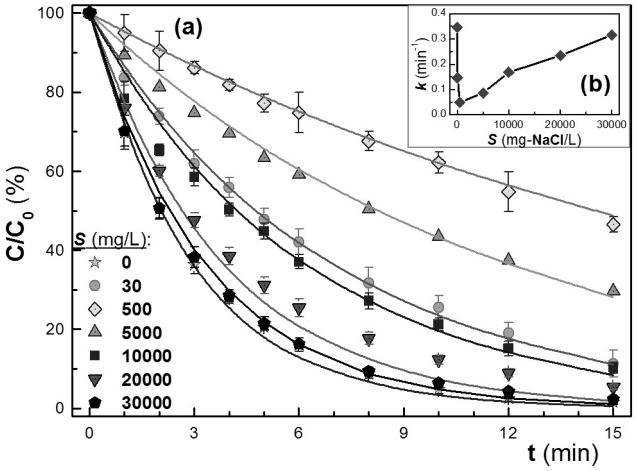

Fig. 3. Degradation of CFA with NaCl: (a) Removal profiles; (b) Dependence of kinetic constant with substrate concentration. Solid curves are calculated by Eq. (3).

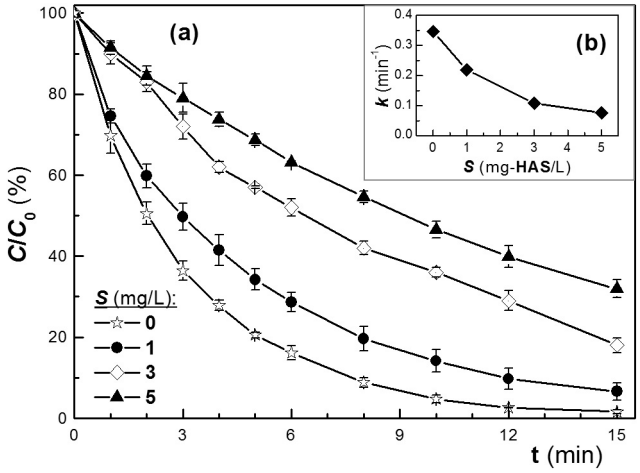

Fig. 4. Degradation of CFA with HAS: (a) Removal profiles; (b) Dependence of kinetic constant with substrate concentration.

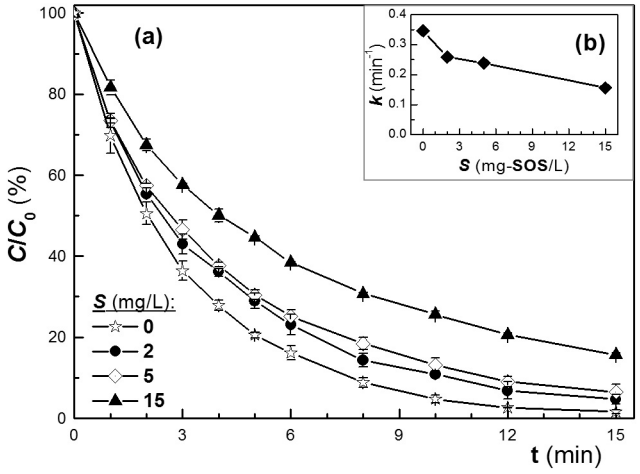

Fig. 5. Degradation of CFA with SOS: (a) Removal profiles; (b) Dependence of kinetic constant with substrate concentration.

expected in the range between pK_a of CFA and pzc of TiO_2. This is consistent with our data in which CFA showed much better degradation rates at acidic conditions.

3.2.1. *Presence of inorganic salts*

As noted in Table 2, a number of assays were carried out to assess the extent of CFA photolysis in water with addition of inorganic salts. Some salts tested have been commonly used as coagulants in WWTPs (iron and aluminium salts), while the others are naturally present in waters. In particular, the effect of sodium chloride was studied over a wide range of concentrations (from freshwater to saltwater). As an example, the removal profiles of CFA with time and the dependence of the observed first-order kinetic constant (k) with the actual concentration of added substrate (S) are given in Fig. 3 for NaCl. The solid curves have been calculated from the proposed kinetic model as will be discussed below. The corresponding results obtained for the other salts are plotted in Figs. A.2–A.10 of the supplementary material (Appendix A). In general, the presence of inorganic salts had a negative effect on the photocatalytic activity of TiO_2 in the degradation of CFA. Thus, generally, the higher the salt concentration, the more the deactivation effect. Two deactivation routes by inorganic anions have been proposed, competition for free radicals and blockage of catalyst active sites by adsorption of anions to form a surrounding layer [24,32]. On the other side, UV-light attenuation did not play a significant role except for Fe^{3+} solutions (yellowish color).

As can be deduced from Table 2, sulfates and carbonates apparently caused a stronger deactivation effect than chlorides. Thus, decreases in CFA degradation of over 70% were observed after 15 min treatment when the former were present. This agrees with the known fact that sulfates and carbonates are both good scavengers of reactive oxygen species. Also as aforementioned, it is remarkable that unlike with the other chloride salts tested, the degradation rates of CFA in presence of $AlCl_3$ were higher or comparable to those measured in pure water (up to 120 mg-$AlCl_3$/L, Fig. S3).

As a noteworthy result, the asymmetric u-shaped curve obtained for the kinetic constant (Fig. 3b) indicates that sodium chloride produces opposite effects depending on the added salt concentration. In this case, aggregation does not seem to be determinant for photocatalytic activity since aggregate sizes with NaCl were high (d> 3500 nm; Table 2) at all of the concentrations studied. At low NaCl concentrations, the degradation of CFA may be slowed down because of adsorption of chlorides on TiO_2 surface which reduces the available catalyst active sites. On the other hand, above 0.05% NaCl, ionic strength has been pointed out as determinant for photocatalytic efficiency [33]. Thus, at high ionic strength, the electric double layer becomes more compressed and thereby decreases the resistance of CFA to reach the catalyst surface making easier its adsorption. Anyway, the degradation profiles observed within 3.0% NaCl and within pure water were so similar (Fig. 3a) which suggests that, under certain conditions, photocatalytic degradation could be efficiently performed in highly saline matrices.

3.2.2. *Presence of organic matter*

Different assays were made to evaluate the photodegradation of CFA when other organic moieties were present, in this case humic acids and sodium n-octylsulfate. Humic acids are common substances derived from organic matter decomposition, so often appear in environmental waters at low concentrations, most often below 10 mg/L [14]. Hence, the photocatalytic degradation of CFA was tested for humic acid sodium salt (HAS). As for natural organic matter, the chemical structure of HAS is not well defined, but a molecular formula of $C_9H_8Na_2O_4$ is commonly taken as representative. Sodium n-octylsulfate (SOS) is an anionic surfactant widely used in cleaning and hygiene products, which is expected it can enter WWTPs in significant concentrations. The results obtained for both HAS and SOS are shown in Figs. 4 and 5. In both cases, but more markedly for HAS, the presence of dissolved organic matter in water clearly diminished the photocatalytic activity by competition

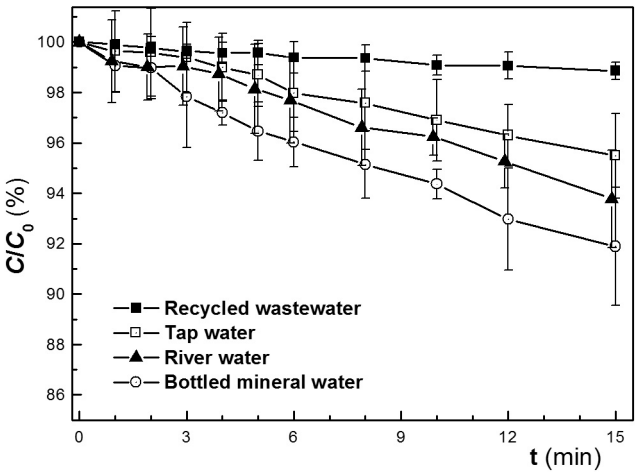

Fig. 6. Degradation profiles of CFA in different environmental waters.

for both active sites and species. Furthermore, UV-light attenuation was observed in HAS solutions in which UV-light absorbances of 20% and 12% were measured for 5 and 3 mg/L, respectively. Also, with the surfactant, the photocatalytic deactivation could be caused by the formation of micelles around CFA and by the presence of sulfates from the photolysis of SOS itself [34,35]. Nevertheless, the surfactant concentrations we used are under its critical micelle concentration (0.142 mol-SOS/L at 30 °C) [34], so competition for active sites and inhibition by sulfate seem to be the main reasons for the catalyst activity loss observed.

3.2.3. *Effect of environmental waters*

Four different types of environmental waters (mineral water, tap water, river water, and recycled wastewater) were used as target matrices. The CFA photodegradation profiles obtained in these waters are shown in Fig. 6. As observed, strong decreases in photocatalytic activity (over 90% after 15 min) were observed with all environmental waters in comparison with pure water. In fact, no significant differences in CFA degradation were found between the relatively clean sources such as tap water (2.2 mg-TOC/L) or bottled mineral water (<0.2 mg-TOC/L) and those with low-medium organic matter content such as river water (4.7 mg-TOC/L) or recycled wastewater (27.1 mg-TOC/L). However, the worst results were obtained with recycled wastewater that was the only matrix in which light attenuation was appreciated (a light absorbance of 37%).

For practical purposes, the catalyst deactivation found in weakly saline waters is attributed to the combined effect of the presence of both the different mineral species and the organic matter. Note that the predominant anions in all of these samples were chlorides, sulfates and carbonates. Thus, the recycled water matrix had appreciable concentrations of alkali-alkaline earth (Ca, Mg and K, between 60 and 180 mg/L) and heavy metals (Al, Fe and Mn, from 50 to 210 μg/L), whilst tap water presented much lower concentrations of all cations except aluminium (67 μg/L). A similar observation was made with an antibiotic photocatalytically treated in a hospital effluent water [36].

3.3. *General kinetic model*

An effort was made to correlate the CFA photodegradation with the type and concentration of each substance added to pure water. The objective was to build a prediction model in which each substance added to form the aqueous matrix could be defined by a single scalar parameter (F) valid for the entire range of concentrations tested. Because of the low ranges used, the concentrations of the spiked compounds (S) were always expressed as mmol/L in the fitting procedure. Unfortunately, the data for HAS could not be included in the analysis because of its molecular weight cannot be defined (a range of 2–500 kDa is reported by the supplier).

Table 4
Results of the global fitting analysis.

Cation	F^+	Anion	F^-
Al^{3+}	−0.2219	Cl^-	−0.05072
Ca^{2+}	0.09448	CO_3^{2-}	3.690
Fe^{3+}	0.1460	HCO_3^-	2.494
Fe^{2+}	0.1124	SO_4^{2-}	1.444
Na^+	−0.07789	SOS^-	0.2552
	k_1	k_2	k_3
a_i	−0.09865	−2.094	5.421
b_i	0.01704	−7.400	6.079
Compound	R^2	Compound	R^2
NaCl	0.9950	$Fe_2(SO_4)_3$	0.9995
$FeCl_3$	0.9766	Na_2SO_4	0.9962
$FeCl_2$	0.9933	$NaHCO_3$	0.9949
$AlCl_3$	0.9963	Na_2CO_3	0.9954
$CaCl_2$	0.9984	SOS	0.9933
$Al_2(SO_4)_3$	0.9976		

Since, a first-order kinetics was deduced from the individual experiments (Eq. (1)), our attention was focused on finding a correlation to predict good values for the kinetic constant (k).

$$C/C_0 = \exp(-k\,t) \tag{1}$$

The shape of the k–S profile for NaCl (Fig. 3b) somewhat resembles a mirror curve of the bacterial growth kinetics with substrate inhibition. So bearing this in mind, different approaches were tried to fit the experimental data. Among them, the best one was provided by a model based on that of Yano-Koga [37]:

$$r_S = r_{Smax} S/(K_S + S + S^3/K_I{}^2) \tag{2}$$

being r_S the specific substrate uptake rate, S substrate concentration, K_S half-saturation constant, and K_I inhibition constant.

Accordingly, the proposed model is defined as:

$$C/C_0 = \exp\left[-k_0(1 - k_1 S/(k_2 + S + S^3/k_3{}^2)t\right] \tag{3}$$

where S is the concentration of the added compound, and the coefficients k_i (i = 1, 2, 3) are constants depending on that compound according to:

$$k_i = \exp\left[(a_i + b_i F)/(1 + F)\right] \tag{4}$$

Notwithstanding, the coefficient F which defines each molecule is not an adjustable parameter of the model as it is defined as a function dependent on its ionic species:

$$F = N_{Z-} F^+ + N_{Z+} F^- \tag{5}$$

being N_{Z+} and N_{Z-} the respective electric charges (absolute values) of the cationic and anionic forms of the substance considered, respectively.

Note that Eq. (4) corresponds to three independent equations, one for each constant k_i in Eq. (3). It is noteworthy that the value for k_0 was set constant and equal to that obtained with pure water (i.e., k_0 = 0.3468 min^{-1}). Thereby, with our data, six parameters from Eq. (4) together with ten characteristic coefficients (one for each ionic species spiked in water, see Table 4) should be calculated in the model. The results of the global fitting analysis are summarized in Table 4, wherein each partial R^2 value corresponds to the particular dataset for each substance listed. Good agreement was observed between experimental CFA concentrations and those predicted by the proposed model (overall R^2 = 0.9947, n = 396), as can be also observed in Fig. A.11. The worst fit was found with $FeCl_3$

(Fig. A.2, $R^2 = 0.9766$). Certainly the individual fittings (by processing the dataset of each substance separately) were still better than global fitting ($R^2 = 0.993$ for $FeCl_3$ in the former case).

The obtained results appear to suggest a certain relationship between the characteristic coefficient defining each substance added (F) and its mean zeta potential value (Z). In fact, strong negative correlations were found for both positive Z values ($r = -0.781$, $p = 0.038$) as for those negative ($r = -0.995$, $p = 0.065$). Nevertheless, the attempts to include the characteristic coefficients F in the model instead of the actually measured Z values were not successful enough, and no clear conclusions could be drawn in this respect. In any case, although further research could be needed to extend the applicability of the proposed model to other common substances and mixtures, the procedure developed is suggested as a general methodology to quantify the deactivation effects by presence of well-characterized substances in photocatalytic systems. It is noteworthy that the form of the general equation (Eq. (3)) is not affected by changes in the experimental arrangement or the target compound. In fact, although the validation has been done for a given compound (CFA), the kinetic model developed here could be easily applied to another solutes by recalculating the fitting coefficients. Note that once the target solute and the catalyst form are defined, the base aqueous matrix would determine the value of k_0 while the other coefficients would depend on the other compounds present in water.

5. Conclusions

Photocatalysis is a promising technique to remove micropollutants from environmental waters. In this study, clofibric acid (CFA) was used as a target compound to study the effect of the water matrix on photodegradation by UV light irradiation. To this aim, five TiO_2-based photocatalysts were tested in pure water and determined the optimal dosage (0.50 g/L) for the one (Aeroxide P25) with the best CFA removal efficiency (>98% after a 15-min treatment). However, when testing unclean water matrices, this efficiency decreased dramatically because of the deactivating effect of organic and inorganic compounds. Among the latter, sulfates and carbonates were found to give the largest efficiency drop (over 70%), whereas the presence of $AlCl_3$ had little effect compared with pure water. Different environmental waters (mineral water, tap water, river water, and recycled wastewater) were evaluated, obtaining even larger efficiency decreases (over 90%), which has been attributed to the combined effect of the presence of salts and organic matter. Finally, a general kinetic model has been purposed to correlate CFA degradation with the type and concentration of any substance present in water. A single parameter is used to characterize each compound spiked to water. The model developed has been successfully applied and it is proposed as a good starting point to determine deactivation effects in another photocatalytic systems.

Acknowledgements

The authors are greatly thankful to the Association of Friends of the University of Navarra for the grant of N. Rioja.

Appendix A. Supplementary data

Supplementary data associated with this article can be found, in the online version, at http://dx.doi.org/10.1016/j.apcatb.2015.06.038

References

[1] B. Halling-Sørensen, S. Nors-Nielsen, P.F. Lanzky, F. Ingerslev, H.C. Holten-Lützhøft, S.E. Jørgensen, Chemosphere 36 (1998) 357–393.
[2] R.P. Schwarzenbach, B.I. Escher, K. Fenner, T.B. Hofstetter, C.A. Johnson, U. Von Gunten, B. Wehrli, Science 313 (2006) 1072–1077.
[3] A.K. Da Silva, J. Amador, C. Cherchi, S.M. Miller, A.N. Morse, M.L. Pellegrin, M.J.M. Wells, Water Environ. Res. 85 (2013) 1978–2021.
[4] W.C. Li, Environ. Pollut. 187 (2014) 193–201.
[5] S.R. Hughes, P. Kay, L.E. Brown, Environ. Sci. Technol. 47 (2013) 661–677.
[6] J. Sánchez-Avila, J. Vicente, B. Echavarri-Erasun, C. Porte, R. Tauler, S. Lacorte, Mar. Pollut. Bull. 72 (2013) 119–132.
[7] Y. Luo, W. Guo, H.H. Ngo, L.D. Nghiem, F.I. Hai, J. Zhang, S. Liang, X.C. Wang, Sci. Total Environ. 473–474 (2014) 619–641.
[8] F. Naitali, H. Ghoualem, Desalin. Water Treat. 52 (2014) 2340–2343.
[9] S. Zorita, L. Martensson, L. Mathiasson, Sci. Total Environ. 407 (2009) 2760–2770.
[10] M. Al Aukidy, P. Verlicchi, A. Jelic, M. Petrovic, D. Barceló, Sci. Total Environ. 438 (2012) 15–25.
[11] P. Verlicchi, M. Al Aukidy, E. Zambello, Sci. Total Environ. 429 (2012) 123–155.
[12] S. Carbonaro, M.N. Sugihara, T.J. Strathmann, Appl. Catal. B 129 (2013) 1–12.
[13] N. De la Cruz, R.F. Dantas, J. Giménez, S. Esplugas, Appl. Catal. B 130–131 (2013) 249–256.
[14] L. Haroune, M. Salaun, A. Ménard, C.Y. Legault, J.P. Bellenger, Sci. Total Environ. 475 (2014) 16–22.
[15] S. Ahmed, M.G. Rasul, R. Brown, M.A. Hashib, J. Environ. Manag. 92 (2011) 311–330.
[16] S.K. Sharma, H. Bhunia, P.K. Bajpai, Clean-Soil Air Water 40 (2012) 1290–1296.
[17] G. Rammohan, M.N. Nadagouda, Curr. Org. Chem. 17 (2013) 2338–2348.
[18] D. Kanakaraju, B.D. Glass, M. Oelgemöller, Environ. Chem. Lett. 12 (2014) 27–47.
[19] D. Friedmann, C. Mendive, D. Bahnemann, Appl. Catal. B 99 (2010) 398–406.
[20] J.M. Herrmann, Appl. Catal. B 99 (2010) 461–468.
[21] J. Olabarrieta, S. Zorita, I. Peña, N. Rioja, O. Monzón, P. Benguria, L. Scifo, Appl. Catal. B 123–124 (2012) 182–192.
[22] M.N. Chong, B. Jin, C.W.K. Chow, C. Saint, Water Res. 44 (2010) 2997–3027.
[23] A.G. Rincón, C. Pulgarin, Appl. Catal. B 51 (2004) 283–302.
[24] C. Guillard, E. Puzenat, H. Lachheb, A. Houas, J.M. Herrmann, Int. J. Photoen. 7 (2005) 1–9.
[25] W.A. Adams, C.A. Impellitteri, J. Photochem. Photobiol. A- Chem. 202 (2009) 28–32.
[26] E. Hapeshi, A. Achilleos, M.I. Vasquez, C. Michael, N.P. Xekoukoulotakis, D. Mantzavinos, D. Kassinos, Water Res. 44 (2010) 1737–1746.
[27] W. Li, S. Lu, Z. Qiu, K. Lin, Ind. Eng. Chem. Res. 50 (2011) 5384–5393.
[28] Z. Frontistis, V.M. Daskalaki, E. Hapeshi, C. Drosou, D. Fatta-Kassinos, N.P. Xekoukoulotakis, D. Mantzavinos, J. Photochem. Photobiol. A- Chem. 240 (2012) 33–41.
[29] N. Rioja, P. Benguria, F.J. Peñas, S. Zorita, Environ. Sci. Pollut. Res. 21 (2014) 11168–11177.
[30] H.R. Jafry, M.V. Liga, Q. Li, A.R. Barron, Environ. Sci. Technol. 45 (2011) 1563–1568.
[31] S. Malato, P. Fernández-Ibáñez, M.I. Maldonado, J. Blanco, W. Gernjak, Catal. Today 147 (2009) 1–59.
[32] O. Carp, C.L. Huisman, A. Reller, Prog. Solid State Chem. 32 (2004) 33–177.
[33] A. Aguedach, S. Brosillon, J. Morvan, E.K. Lhadi, J. Hazard. Mater. 150 (2008) 250–256.
[34] K. Ogino, T. Kakihara, M. Abel, Colloid Polym. Sci. 265 (1987) 604–612.
[35] H. Hidaka, K. Nohara, K. Ooishi, J. Zhao, N. Serpone, E. Pelizzetti, Chemosphere 29 (1994) 2619–2624.
[36] X. Van Doorslaer, J. Dewulf, J. De Maerschalk, H. Van Langenhove, K. Demeestere, Chem. Eng. J. 261 (2015) 9–16.
[37] T. Yano, S. Koga, Biotechnol. Bioeng. 11 (1969) 139–153.